A Three-Dimensional Numerical Study into Non-Axisymmetric Perturbations of the Hole-Tone Feedback Cycle

Mikael A. LANGTHJEM, Masami NAKANO

Department of Mechanical Systems Engineering, Faculty of Engineering, Yamagata University, Jonan 4-chome, Yonezawa-shi, 992-8510 Japan

Abstract. This work is concerned with the hole-tone feedback cycle problem, also known as Rayleigh's bird-call. A simulation method for analyzing the influence of non- axisymmetric perturbations of the jet on the sound generation is described. In planned experiments these perturbations will be applied at the jet nozzle via piezoelectric or electro-mechanical actuators, placed circumferentially inside the nozzle at its exit. The mathematical model is based on a three-dimensional vortex method. The nozzle and the holed end-plate are represented by quadrilateral vortex panels, while the shear layer of the jet is represented by vortex rings, composed of vortex filaments. The sound generation is described mathematically using the Powell-Howe theory of vortex sound. The aim of the work is to understand the effects of a variety of flow perturbations, in order to control the flow and the accompanying sound generation.

Keywords: aeroacoustics; self-sustained flow oscillations; three-dimensional vortex method

1. Introduction

Self-sustained fluid oscillations can occur in a variety of practical applications where a shear layer impinges upon a solid structure [1]. The oscillations are the cause of sound generation, which typically is powerful. In cases of music instruments (flutes, etc.) and whistles, sound generation is, of course, the aim. By engineering applications however, the sound generation is, in most cases, an unwanted, annoying side effect.

The present paper is concerned with the so-called hole-tone problem [2, 3]. The common teakettle whistle is an example of utilization of the sound generation in this system. The steam jet, issuing from a nozzle, passes through a similar hole in a plate, placed a little downstream from the nozzle. The shear layer of the jet is unstable and rolls up into a large, coherent vortex ('smoke-ring'). This large vortex cannot pass through the hole in the plate and hits the edge of the hole, where it creates a pressure disturbance. This disturbance is thrown back (with the speed of sound) to the nozzle, where it disturbs the shear layer. This initiates the roll-up of a new coherent vortex. In this way an acoustic feedback loop is formed. Figure 1(a) illustrates the principle of the hole-tone phenomenon. Figure 1(b) shows an experimental realization, with the vortex roll-up visualized by the smoke wire technique [4].

The basic dynamics of the hole-tone feedback system was studied numerically in Ref. [5], using an axisymmetric discrete vortex method, combined with an aeroacoustic model based on Curle's theory [6]. This approach could predict the fundamental

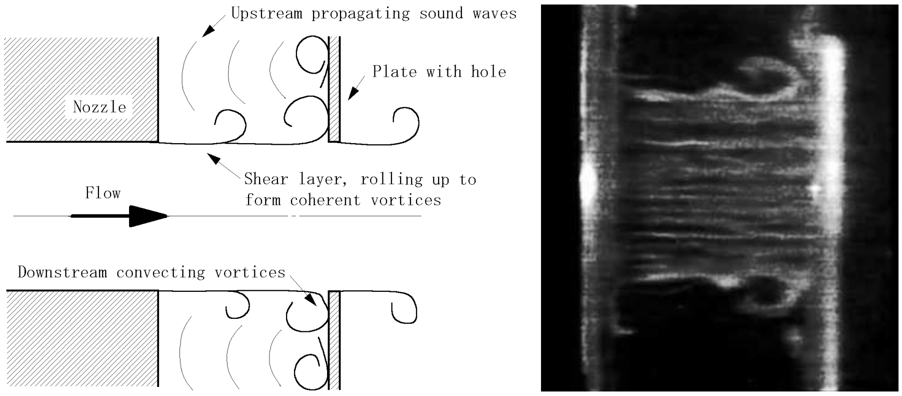

Figure 1. Left: Geometry and physical features of the hole-tone problem. Right: Flow visualization of the vortex roll-up [4].

characteristics of the problem quite well, in particular the fluid-dynamic characteristics. The acoustic model gave qualitative correct results but overestimated the sound pressure levels.

The hole-tone system is a part of many engineering systems, where sound generation is unwanted. Examples include automobile intake- and exhaust systems, gas/steam distribution systems (bellows, valves, etc.), and solid-propellant rocket motors. In these cases, if a geometry which avoids the sound-generation cannot easily be obtained, a control method which can eliminate, or at least suppress, the sound generation is desirable.

Nakano *et al.* [4] studied experimentally a forced excitation strategy to eliminate the hole-tone feedback cycle in the system depicted in Figure 1. The shear layer near the nozzle exit was acoustically excited by means of an excitation chamber equipped with six loudspeakers, placed equidistantly around the circumference. By harmonic excitation at frequencies away from the fundamental frequency f_0, noise level reductions (at f_0) of up to 6 dB were achieved.

The aim of the present work is to develop a numerical method for simulating the hole-tone problem with the jet subjected to *non-axisymmetric* 'mechanical' ('non-acoustic') perturbations, by piezoelectric or electro-mechanical actuators mounted at the nozzle exit, similar to the concept of Kasagi [7]. This is expected to be more efficient than acoustic perturbations [4], and the aim is to study/verify this carefully before experimental verification, using a three-dimensional vortex method.

2. Flow Model

The shear layer of the jet issuing from the nozzle is represented in a lumped form, by a 'necklace' of discrete vortex rings. These rings are disturbed mechanically at the nozzle exit such that they loose their natural axisymmetric form, and are thus represented by three-dimensional vortex filaments. The induced velocity $\mathbf{u}_i = (u_1, u_2, u_3)_i$, at position $\mathbf{x}_i = (x_1, x_2, x_3)_i$ and time t, from J vortex rings represented by the space curves $\mathbf{r}_j(\xi, t)$, is given by

$$\mathbf{u}_i(\mathbf{x}_i, t) = -\sum_{j=1}^{J} \frac{\Gamma_j}{4\pi} \int_\xi \frac{\{\mathbf{x}_i(t) - \mathbf{r}_j(\xi, t)\} \times \partial \mathbf{r}_j / \partial \xi}{\{|\mathbf{x}_i(t) - \mathbf{r}_j(\xi, t)|^2 + \alpha \sigma_j^2(\xi, t)\}^{\frac{3}{2}}} d\xi, \tag{1}$$

where Γ_j is the strength (circulation) of the j'th vortex, ξ is a material (vortex) coordinate, and $\sigma_j(\xi, t)$ is the core radius. The parameter α represents the vorticity distribution within the core; for a Gaussian distribution, $\alpha \approx 0.413$.

The space curves $\mathbf{r}_j(\xi, t)$ are discretized by employing K marker points on each curve (vortex ring), connected via cubic splines or, optionally, via straight segments. The integration in (1) is carried out using Gauss-Legendre quadrature when splines are used, and analytically when straight segments are used.

A vortex ring is released from the nozzle at each time step in the simulation. [Earlier studies [5] have shown that the vortex shedding from the edge of the hole in the end plate is insignificant.] The strength of the vortex ring to be released is dictated by the Kutta condition.

The convection velocity of a shed vortex ring is dictated by the induced velocities from all other vortex rings, plus the self-induced velocity, as indicated by (1). The positions $\mathbf{r}_i$ of the shed vortex filament ring marker points are updated by solving numerically the system of ordinary differential equations $\mathrm{d}\mathbf{r}_i(t)/\mathrm{d}t = \mathbf{u}_i(\mathbf{r}_i, t)$.

The solid surfaces are represented by quadrilateral vortex panels, made up of four straight vortex filaments, as indicated in Fig. 2. The inviscid boundary condition of zero normal velocity is imposed at control points in the center of these panels. The mean jet flow is provided by a number of panels placed on the 'back' of the nozzle tube; see again Fig. 2. The strengths of the bound vortex panels are dictated by the boundary conditions and by the mean jet velocity. The mechanical/piezoelectric actuator system is simulated by periodical 'edge wave' deformations of the nozzle end section, as illustrated also by Fig. 2.

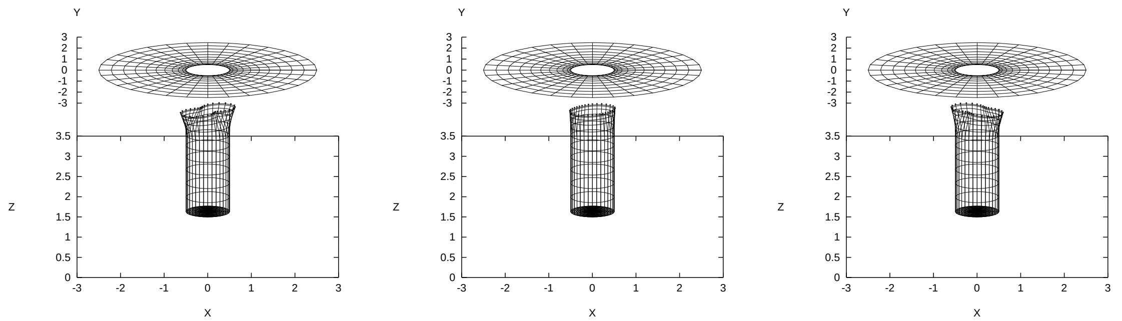

Figure 2. Illustration of the perturbation mechanism (actuator model). [For purpose of illustration the amplitude is exaggerated.]

3. Aeroacoustic Model

The theory of vortex sound is applied to compute the sound generation. For low Mach-number flows it is described by the inhomogeneous wave equation

$$c_0^{-2}\partial^2 p/\partial t^2 - \nabla^2 p = \rho_0 \nabla \cdot \mathbf{L}, \tag{2}$$

where $p(\mathbf{x}, t)$ is the acoustic pressure, $\mathbf{L} = \boldsymbol{\omega} \times \mathbf{u}$ is the Lamb vector, with the vorticity $\boldsymbol{\omega}$ given by $\nabla \times \mathbf{u}$; ρ_0 is the mean air density, and c_0 the speed of sound.

In the present work (2) is solved in two different ways: (i) by using the compact Green's function approach; (ii) by using the boundary element method. A detailed description of approach (i) can be found in e.g. [6]; accordingly only approach (ii) will be described here.

Based on the free space Green's function the solution to (2) can be expressed as

$$p(\mathbf{x},t) = p_v(\mathbf{x},t) + \frac{1}{4\pi}\iint_{S_b}\left\{[\tilde{p}]_{t_r}\frac{\partial}{\partial n_b}\left(\frac{1}{r_{xb}}\right) - \left[\frac{\partial \tilde{p}}{\partial t}\right]_{t_r}\frac{1}{c_0\, r_{xb}}\frac{\partial r_{xb}}{\partial n_b}\right\} dS, \tag{3}$$

where $\tilde{p}$ indicates the pressure difference across the end plate, $\iint_{S_b}\ldots dS$ denotes integration over *one* surface, and $r_{xb} = |\mathbf{x} - \mathbf{x}_b|$ is the distance between the observation point $\mathbf{x}$ and a point $\mathbf{x}_b$ on the end plate. The normal vector at $\mathbf{x}_b$ is denoted by n_b. Square brackets with subscript t_r indicate evaluation at the retarded time $t_r = t - |\mathbf{x} - \mathbf{x}_b|/c_0$. The 'source term' $p_v(\mathbf{x},t)$ is given by

$$p_v(\mathbf{x},t) = -\frac{1}{4\pi}\iiint_{\mathbf{y}}\left[L_j(\mathbf{y},t_r)\frac{x_j - y_j}{r_{xy}^3} + \frac{\partial L_j}{\partial t}(\mathbf{y},t_r)\frac{x_j - y_j}{c_0\, r_{xy}^2}\right]_{t_r} d^3\mathbf{y}, \tag{4}$$

where summation over repeated subscript j's applies. The pressure difference $\tilde{p}$ is determined from the equation [9]

$$\frac{\partial p_v}{\partial n_a}(\mathbf{x}_a,t) + \iint_{S_b}\left\{[\tilde{p}]_{t_r}\frac{\partial^2}{\partial n_a \partial n_b}\left(\frac{1}{r_{ab}}\right) - \left[\frac{\partial \tilde{p}}{\partial t}\right]_{t_r}\frac{1}{c_0 r_{ab}}\frac{\partial^2 r_{ab}}{\partial n_a\, \partial n_b}\right\} dS = 0, \tag{5}$$

Equations (3) and (5) are discretized via the boundary element method.

4. Numerical Example and Concluding Remarks

Computations are carried out for a setup with nozzle and end plate hole diameter d_0 equal to 50 mm. The outer diameter of the end plate is 250 mm. The gap length L is 50 mm, e.g., equal to d_0. The mean velocity u_0 of the air-jet is 10 m/s. At 20 °C this corresponds to a Reynolds number $Re = u_0\, d_0/\nu \approx 3.3 \times 10^4$ and a Mach number $M = u_0/c_0 \approx 0.03$, where the speed of sound $c_0 = 340$ m/s and the kinematic viscosity $\nu = 1.5 \times 10^{-5}$ m^2/s. A number of side view 'snapshots' of the jet during approximately one period os oscillation are shown in Fig. 3. The computed fundamental frequency $f_0 \approx 190$ Hz, which is quite close to the experimentally observed value of 196 Hz.

The influence of nozzle-oscillations is exemplified by Fig. 4 which shows the sound pressure levels (in dB) midway between nozzle exit and end plate, five nozzle diameters away from the central axis. Part (a) is for the case without nozzle oscillations. part (b) is for a case where the radius of the nozzle, in polar coordinates, is given by $r(\theta,z) = r_0(1 + \epsilon\sin(2\theta)\cos(2\pi f_d t)(1 + z/r_0))$, $0 \le \theta \le 2\pi$, $-r_0 \le z \le 0$ (with nozzle exit at $z = 0$), $\epsilon = \frac{1}{60}$, and $f_d = 300$ Hz. It is expected that the oscillating nozzle can destroy the coherence of the 'smoke rings' and thus decrease the noise generation. In the present example the noise level has however been significantly increased, with the largest component at $f \approx f_d/2$. It is thus clear that appropriate choices of amplitudes, modes and frequencies are very important in controlling the hole-tone feedback cycle.

Acknowledgement. The support of the present project through a JSPS Grant-in-Aid for Scientific Research (No. 18560152) is gratefully acknowledged.

References

[1] Rockwell, D., Naudascher, E., Self-sustained oscillations of impinging free shear layers. *Annu. Rev. Fluid Mech.* **11** (1979) 67-94.

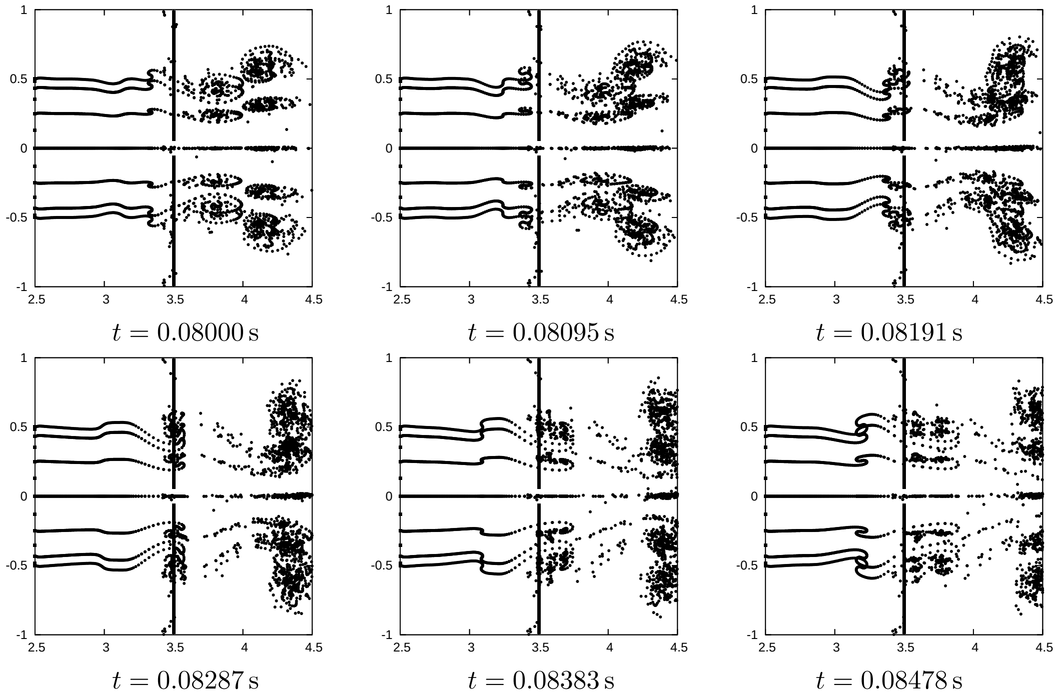

Figure 3. Side view of the jet during approximately one period of oscillation. The nozzle exit is at the abscissa position 2.5; the end plate with hole at position 3.5.

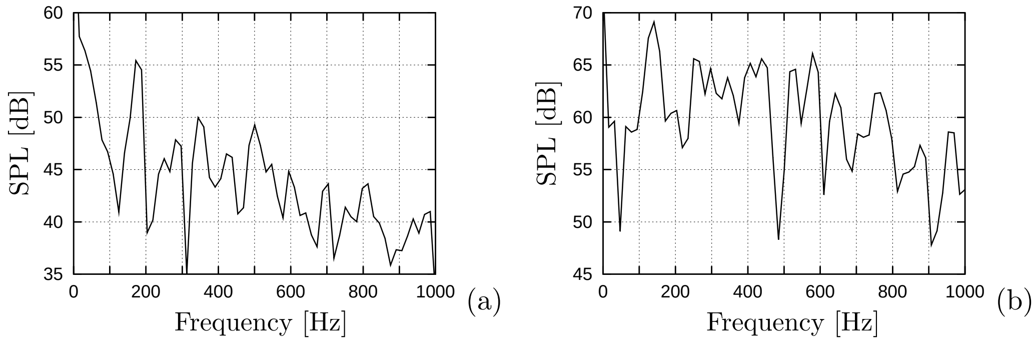

Figure 4. Sound pressure levels (a) without and (b) with nozzle oscillations.

[2] Lord Rayleigh, *The Theory of Sound*, Vol. II, Dover Publications, (1896, re-issued 1945).

[3] Chanaud, R.C., Powell, A., Some experiments concerning the hole and ring tone. *J. Acoust. Soc. Am.* **37** (1965) 902-911.

[4] Nakano, M., Tsuchidoi, D., Kohiyama, K., Rinoshika,A., Shirono, K., Wavelet analysis on behavior of hole-tone self-sustained oscillation of impinging circular air jet subjected to acoustic excitation, (In Japanese) *Kashikajouhou* **24** (2004) 87-90.

[5] Langthjem, M.A., Nakano, M., A numerical simulation of the hole-tone feedback cycle based on an axisymmetric discrete vortex method and Curle's equation. *J. Sound and Vibr.* **288** (2005) 133-176.

[6] M. S. Howe, *Theory of Vortex Sound*, Cambridge Univ. Press, (2003).

[7] Kasagi, N., Toward smart control of turbulent jet mixing and combustion, *JSME Int., J. Ser. B* **49** (2006) 941-950.

[8] Cottet, G.-H., Koumoutsakos, P.D., *Vortex Methods: Theory and Practice*, Cambridge Univ. Press, (2000).

[9] Kawai, Y., Terai, T., A numerical method for the calculation of transient acoustic scattering from thin rigid plates. *J. Sound and Vibr.* **141** (1990) 83-96.